Analyst

Accepted Manuscript

ROYAL SOCIETY OF CHEMISTRY

www.rsc.org/analyst

Journal Name

RSCPublishing

ARTICLE

^{13}C-Engineered Carbon Quantum Dots for in vivo Magnetic Resonance and Fluorescence Dual-Response

Cite this: DOI: 10.1039/xoxxoooooox

Yang Xu, [a] Yu-Hao Li, [b] Yue Wang, [b] Jian-Lin Cui, [b] Xue-Bo Yin, [a,] * Xi-Wen He, [a] and Yu-Kui Zhang [a,c]

Received ooth January 2012,
Accepted ooth January 2012

DOI: 10.1039/xoxxoooooox

www.rsc.org/

Abstract: ^{13}C-engineered carbon quantum dots (^{13}C-QDs) were used as magnetic resonance (MR) and fluorescence dual-response probe. The enhanced ^{13}C-MR signal was observed at 171 ppm from carboxylic and carboxyl carbons in ^{13}C-QDs with 160-fold improvement on signal-to-noise ratio even no hyperpolarization was applied, whereas the intrinsic fluorescence of C-QDs was still kept. The stable MR and fluorescence dual-response was successfully used for long-term observation of zebrafish embryonic development. Cross-validation between MR and fluorescence confirmed the distribution of ^{13}C-QD in zebrafish. ^{13}C-MR provides specific information about the presence, magnitude, and progression of ^{13}C-QDs by defining MR intensity, whereas fluorescence reveals the location of ^{13}C-QDs with its high sensitivity. ^{13}C-MR and fluorescence was observed simultaneously within ^{13}C-QDs and this work may expand the applications of isotope-engineered nanomaterials.

Introduction

The design and development of multimodality probes are critical for molecular diagnosis because multimodality techniques have the complementary and cross-validation ability. [1] Magnetic resonance (MR) has high tissue penetration and limited sensitivity; optical methods are considered to be highly sensitive with less tissue penetration. MR-optical dual-modality technique has therefore attracted much attention. [1] Compared with ^{1}H-MR, ^{13}C-MR has low background because of the low natural abundance of ^{13}C. [2] ^{13}C-labeled molecular probes were therefore used for ^{13}C-MR related applications; MR source in those molecular probes was mainly limited to carboxylic and carboxyl carbons because of low interference in this chemical shift region. [2] To improve the low sensitivity of ^{13}C-MR, hyperpolarization methods, including dynamic nuclear polarization, have been used. [3]

The MR signal derived from carboxylic and carboxyl carbon in hyperpolarized ^{13}C-labeled molecular probes has been used to reveal metabolic pathway [3] and to survey the chemical status of living systems. [2,4] However, hyperpolarized magnetization probes have a longitudinal relaxation time less than 1 min. [2-4] Short decay time hinders the hyperpolarized probes for long-term observation of tissue change. [4b] Moreover, hyperpolarization requires low temperature, high magnetic field, and radioactive materials, which also limit the widespread application of hyperpolarized probes. [3] If the MR sensitivity of a ^{13}C-probe can be improved than that in molecular probes, the conditions for hyperpolarization may be not required.

Carbon quantum dots (C-QDs) are quasi-spherical carbon material with diameters below 10 nm; C-QDs are becoming a promising alternative to metal-based QDs (M-QDs) and dye probes because of their biocompatibility, low toxicity, simple preparation, and favorable luminescence properties. [5] Quantum confinement endows C-QDs size- and wavelength-dependent luminescence and low photo-bleaching. [5] Importantly, C-QDs contain abundant carboxylic and carboxyl carbons. [5-6] If ^{13}C can be integrated into C-QDs, the carboxylic and carboxyl carbons in C-QDs can be used as a ^{13}C-MR source. Compared with the molecular probes, while ^{13}C-labeled C-QDs show MR response, the intrinsic fluorescence of C-QDs is an added bonus. MR and fluorescence dual-response is therefore observed.

We here reported the first ^{13}C-engineered QDs (^{13}C-QDs) for simultaneous *in vivo* MR and fluorescence emission dual-response. To our knowledge, it was the first example of the synergistic combination of ^{13}C-magnetic resonance spectroscopy (MRS) and fluorescence imaging of C-QDs. As validated with zebrafish (*Danio rerio*), ^{13}C-MRS provides specific information about the presence, magnitude, and progression of ^{13}C-QDs by defining MR intensity, whereas fluorescence reveals the location of ^{13}C-QDs with its high sensitivity. As ^{13}C-rich probe, ^{13}C-QDs show 160-fold improvement on the signal-to-noise ratio (SNR) for the peak at around 171 ppm even though hyperpolarization is not applied. So, the lifetime of ^{13}C-MR response is unlimited, while low temperature, high magnetic field, and radioactive materials for hyperpolarization are not required. Different to ^{13}C-labeled molecular probes, [2-4] ^{13}C-QDs are ^{13}C-rich probe for the

improved MR sensitivity. ^{13}C is a stable isotope, so ^{13}C-QDs exhibit the dual-response without engendering radioactive safety concerns. Therefore, ^{13}C-QDs not only expand the utility of C-QDs, but also exhibit the advantages of isotope-engineered nanomaterials for future potential applications.

Results and discussion

Preparation and characterization of ^{13}C-QDs

^{13}C-QDs were prepared by hydrothermal treatment of ^{13}C-glucose. Similarly, ^{12}C-QDs were synthesized using ^{12}C-glucose as a comparison. [7] Their morphology and size were characterized using transmission electron microscopy (TEM). The size distribution of both of C-QDs was mainly focused in the range of 2–6 nm with the average diameters of 3.88 and 3.95 nm, respectively (Fig. 1A and 1B). High-resolution TEM images show that both of C-QDs have the lattice spacing of 0.25 nm (inset in Fig. 1A) for the (100) facet of graphite and illustrate the graphitic structure of C-QDs.[8] ^{13}C- and ^{12}C-QDs have the same average hydrodynamic diameters of 8 nm (Fig. 1C). X-ray photoelectron spectroscopy (XPS, Fig. S2) illustrated the same group types in both C-QDs. Thus, ^{13}C- and ^{12}C-QDs are almost same in the size and morphology because they were prepared with the same carbon source even with different isotopes.

Their fluorescence and UV–vis absorption spectra illustrated the optical properties of ^{13}C- and ^{12}C-QDs (Fig. 1D). The absorptions at 280-320 nm were attributed to the π–π* transition of the aromatic sp^2 domain. [9] Thus, polymerization occurs to form sp^2 carbons in both ^{13}C- and ^{12}C-QDs. Excitation-dependent luminescence was observed from both of C-QDs. Upon excitation from 340 to 480 nm, the emission was observed around 480 nm with the strongest emission at 400 nm excitation (Fig. 1D). Quantum yield was calculated to be 12.7 % for ^{12}C-QDs and 17.1 % for ^{13}C-QDs (Fig. S4 and Table S2). Upconversion emission was observed from two kinds of C-QDs (Fig. S5). ^{13}C-QDs also exhibited excellent resistance to photo-bleaching under continuous UV light excitation within at least 60 min; the emission from ^{13}C-QDs was observed to be stable in salt solution up to 1 M NaCl (Fig. S6), which implied that ^{13}C-QDs would not exhibit significant signal decay over long illumination times and changed salt concentrations for imaging application.

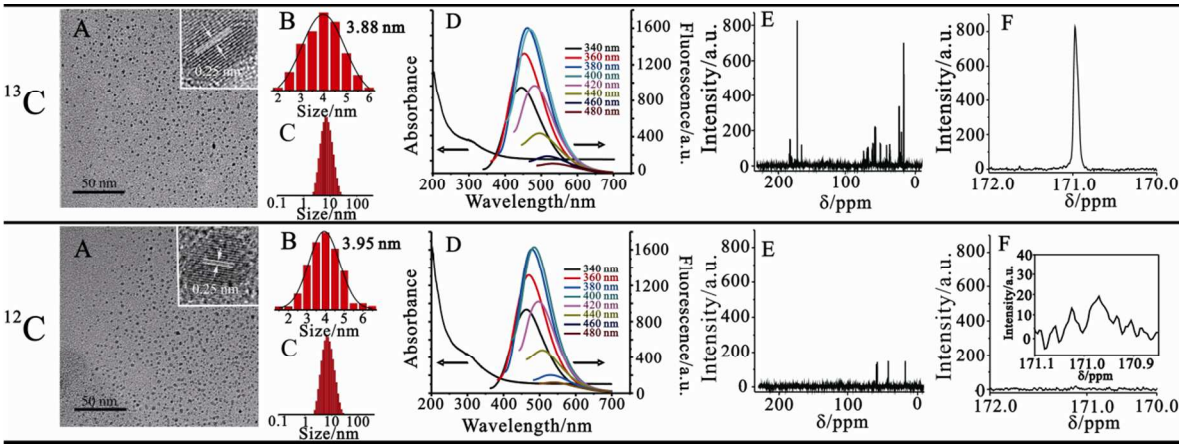

Fig. 1. (A) Transmission electron microscopy (TEM) images (Inset: high resolution TEM images), (B) size distribution, (C) hydrodynamic diameter distribution, (D) absorption and fluorescence spectra using different excitation wavelengths, and (E, F) MR spectra of (upper) ^{13}C-QDs and (lower) ^{12}C-QDs. All of test conditions were same for ^{13}C-QDs and ^{12}C-QDs.

Significantly enhanced magnetic resonance spectroscopy (MRS) and fingerprint information were observed from ^{13}C-QDs (Fig. 1E and 1F). ^{13}C-MRS can distinguish sp^3 carbon from sp^2 carbon and reveal the binding mode in C-QDs.[10] The peaks in the range of 0–50 ppm (Fig. 1E) were attributed to aliphatic (sp^3) carbon. The multiplex signal around 60–75 ppm was related to ^{13}C-spin-splitting of the adjacent ^{13}C in ^{13}C-QDs, but was not observed in ^{12}C-QDs. The responses between 100–150 ppm (Fig. 1E) were ascribed to the internal sp^2 carbon (C=C bond) whereas the peaks at 120–130 ppm most likely arose from polycyclic aromatic carbons. [9,11] The peaks at 170–180 ppm were associated with carboxylic, carboxyl, and amide carbons, showing the surface groups of ^{13}C-QDs. [9,11] All of the results reveal that C-QDs comprise a nanocrystalline core featuring graphitic sp^2 carbon and a surface functionalized with carboxylic/carbonyl groups. [12] It was noteworthy that the peak at 171 ppm in MRS from ^{13}C-QDs was 160-fold improvement in SNR than that from ^{12}C-QDs (Fig. 1F). This signal derived from carboxylic and carboxyl carbons in ^{13}C-QDs and can be used as MR tag, similar to ^{13}C-label molecular probes, where most of ^{13}C unit was limited to carboxyl carbon. [2]

MR and fluorescence responses of ^{13}C-QDs in embryos

Zebrafish are widely used for basic and applied researches such as disease progression, developmental mechanism and pattern formation because of its well-defined developmental stages, and amenability to optical imaging. [12] Zebrafish embryos were first used to validate the ^{13}C-MRS/fluorescence dual-response

of ^{13}C-QDs. After embryos were incubated with ^{13}C-QDs, the bright-field images of embryos were the same to each other, indicating the high biocompatibility (Fig. 2A); ^{13}C-QDs also show low cytotoxicity and biological toxicity (Fig. S7-S9). Their fluorescence images became brighter while the intensity at 171 ppm in MRS increased gradually, without significant change in chemical shift along with increased ^{13}C-QDs concentration (Fig. 2B and 2C). Different brightness between yolk sac and inner mass indicated that ^{13}C-QDs have different affinity to these tissues (Fig. 2B). Thus, ^{13}C-QDs can enter into the embryos across chorion and germ ring. As the first barrier between embryos and allogenic materials, chorion has nanoscale pores (ca. 0.17 μm^2), [13] that is larger than the size of ^{13}C-QDs (ca. 4 nm). Therefore, ^{13}C-QDs can enter into embryo through the pores in the chorion, and then diffuse in the whole embryos. Cheng et al [13] investigated the effect of carbon nanotubes (CNTs) on embryonic development and found CNTs aggregated at the chorion surface owing to their big size. C-QDs are therefore suitable for imaging application because of their smaller size for higher permeability.

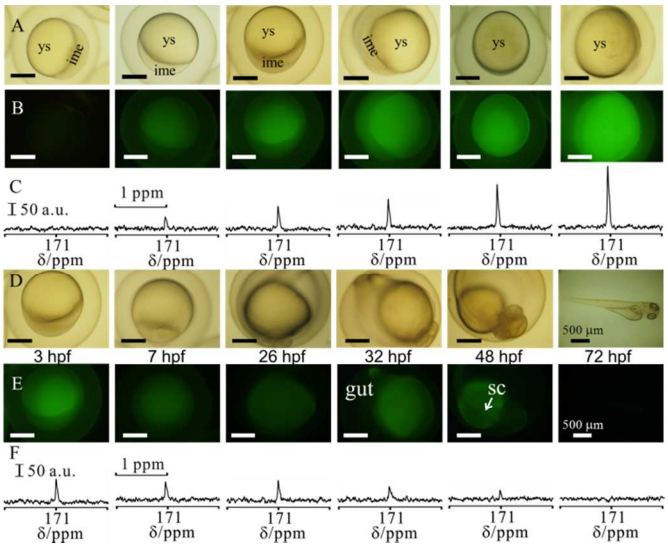

Fig. 2. (A) Bright field images, (B) fluorescence images, and (C) MR spectra of zebrafish embryos incubated with ^{13}C-QDs at different concentrations: 0, 0.5, 1.0, 1.5, 3.0, and 5.0 mg mL^{-1}. (D) Bright field images, (E) fluorescence images, and (F) MR spectra of embryo incubated in 1 mg mL^{-1} ^{13}C-QDs at different stages. Yolk sac: ys, inner mass of embryos: ime, spinal cord: sc. Scale bar: 250 μm besides the marked.

The effect of ^{13}C-QDs on embryonic development was tested after embryos were incubated with ^{13}C-QDs. The embryos underwent rapid cell division to form different organs (Fig. 2D), the same as the untreated embryos as observed in Fig. S9. Both ^{13}C-MR signal and fluorescence were observed from embryos incubated with ^{13}C-QDs, but the intensities decreased gradually along with the embryonic development and disappeared at 72 hpf (Fig. 2E and 2F). Cross-validation is therefore achieved between ^{13}C-MRS and fluorescence of ^{13}C-QDs. Because of their high photo-stability in salt solution (Fig. S6), ^{13}C-QDs may be removed from embryos by the digestive system, as illustrated by the bright gut at 32 hpf (Fig. 2). Moreover, ^{13}C-QDs were transferred to the dorsal from yolk sac as the bright spinal cord in their fluorescence image at 48 hpf (Fig. 2E). ^{13}C-QDs redistributed in the trunk of zebrafish and revealed spatial-temporal progression of embryonic development by their stable fluorescence emission. The unlimited MR lifetime of ^{13}C-QDs also exhibited the temporal progression of zebrafish embryonic development events and therefore ^{13}C-QDs are suitable for long-term observation different to hyperpolarized ^{13}C-label molecular probes (Fig. 2F). [2b]

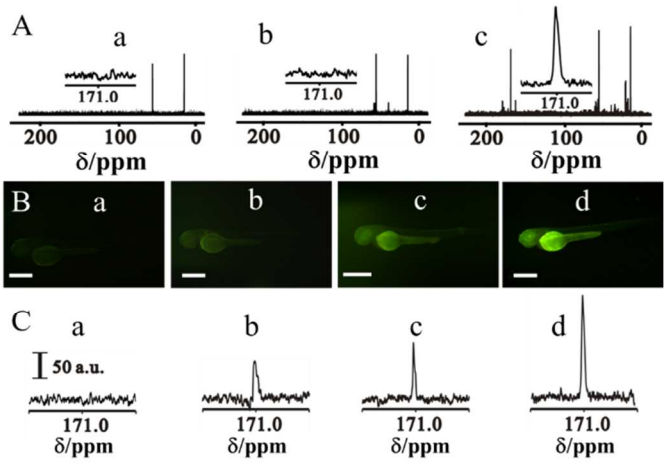

Fig. 3. (A) MR spectra of (a) zebrafish and the zebrafish incubated with 3.0 mg mL^{-1} (b) ^{12}C-QDs and (c) ^{13}C-QDs. Inset: MR signal at around 171 ppm. (B) Fluorescent images and (C) MR spectra of zebrafish incubated with ^{13}C-QDs at different concentration, (a) 0, (b) 0.75, (c) 1.5, and (d) 3.0 mg mL^{-1}. Scale bar: 200 μm.

In vivo MR and fluorescence response of ^{13}C-QDs in zebrafish

The dual-response property of ^{13}C-QDs was further confirmed in zebrafish model. Two peaks appeared at less than 100 ppm in zebrafish MRS even without C-QDs treatment (Fig. 3A). After being incubated with ^{13}C-QDs, the MR fingerprint information of ^{13}C-QDs was clearly evident, besides the peaks from zebrafish as compared with Fig. 3Ac and 1E. The signal intensity at 171 ppm became higher and higher as the concentration of ^{13}C-QDs increased and had no change in chemical shift (Fig. 3C), indicating ^{13}C-QDs in zebrafish were stable. The actual uptake amount of ^{13}C-QDs by zebrafish was ca. 12 μg per fish incubated in 3 mg/mL solution. However, no the signal was observed from the zebrafish incubated with ^{12}C-QDs (Fig. 3Ab), validated the different *in vivo* MR response of ^{12}C- and ^{13}C-QDs (Fig. 3A). Fluorescence images of zebrafish also became brighter and brighter in a concentration-dependent mode (Fig. 3B). The results indicate that fluorescence and MR dual-response of ^{13}C-QDs were maintained even though they were embedded into zebrafish body. The signal from aliphatic carbon less than 100 ppm was observed in the MRS of zebrafish even no C-QDs were embedded in zebrafish, but almost no signal was observed around 171 ppm. Thus, carboxylic and carboxyl carbons are selected as MR source as less interference was observed from tissue. [2]

The absorption, distribution, metabolism and excretion (ADME) of ^{13}C-QDs in zebrafish can be used to understand their potential application and toxicity. The different brightness in zebrafish can be used to illustrate the distribution of ^{13}C-QDs (Fig. 3B and Table S4). After ^{13}C-QDs entered into zebrafish through swallowing and skin-absorption, [14] we found they accumulated selectively in the head, yolk sac, and tail and showed tissue-dependent affinity (Fig. 4 and Table S3). The bright dorsal aorta indicated that ^{13}C-QDs can enter into the circulatory system (Fig. 4G) for the transportation of ^{13}C-QDs. Interestingly, zebrafish eye was the brightest part of head and confirmed by the MR response of ^{13}C-QDs (Fig. 4H and 4I); its brightness increases with the increased ^{13}C-QDs concentrations (Table S3). The lens can be easily distinguished from the eyeball. This result indicates that ^{13}C-QDs can enter the eye across blood-ocular barrier (BOB). Strong fluorescence and MR response was observed from the yolk sac and validated the high content of ^{13}C-QDs in yolk sac (Fig. 4F and 4I).

The ADME route of ^{13}C-QDs was therefore proposed based on their distribution. ^{13}C-QDs enter into yolk sac and are excreted partly through the gut. Some ^{13}C-QDs enter into the cardiovascular system and are transferred throughout the whole body, as illustrated by the brightness in the blood vessel and the tissue in the tail. This result implies that ^{13}C-QDs are a kind of biocompatible probe without apparent quenching and suitable for *in vivo* imaging. [15] Zebrafish has high homology with mammals; the results obtained from zebrafish may therefore be used to model biological effects in other higher animals. [13b] The imaging applications in zebrafish support the promising use of ^{13}C-QDs in clinical application as a low toxicity probe (Fig. S7 and S8).

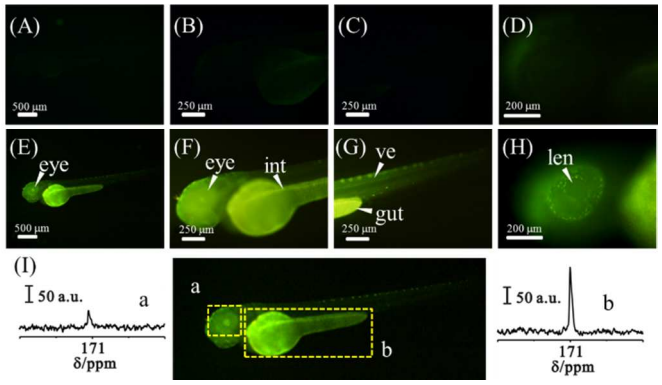

Fig. 4. Fluorescent images of zebrafish (A-D) before and (E-H) after incubated with 3 mg mL^{-1} ^{13}C-QDs. (A, E) Whole zebrafish. (B, F) Front part of body with head and yolk sac. (C, G) Rear part of body. (D, H) Enlarged images of the eye. The eye, tail, yolk sac (ys), intestine (int), vessel (ve), gut and lens (len) were highlighted in the images of the zebrafish incubated with ^{13}C-QDs. (I) MR spectra at 171 ppm of (a) eye and (b) yolk sac in zebrafish.

Morphology of zebrafish illustrated with ^{13}C-QDs

The fluorescence and distribution of a probe can be used to illustrate the morphogenesis and shape of organisms. [16] Confocal images of different scan planes with ^{13}C-QDs as probe clearly show the morphology of zebrafish (Fig. 5 and S10, Movie 1 and 2). The ^{13}C-QDs preferentially accumulate in a very thin layer at the periphery of the zebrafish, confirming that skin-absorption may be one important route by which ^{13}C-QDs enter into zebrafish. The contour of the zebrafish is therefore clearly outlined by the emission of ^{13}C-QDs. The images of the yolk sac of different planes show its scrotiform structure and the intestine is attached to the wall, but not directly to the cavity of the yolk sac. Interestingly, the heart of the zebrafish is observed and the other viscera are also clearly evident in Fig. 5. Thus, the pathway that the fluorescent ^{13}C-QDs enter into the internal of zebrafish through blood circulation is proposed as follows. [12a] The ventral aorta carries blood containing ^{13}C-QDs from the heart into the carotid arteries. Then, part of ^{13}C-QDs is transported into the head through an internal carotid artery; some ^{13}C-QDs enter into dorsal vessels through the ventral aorta. [17] The ^{13}C-QDs are added to the other viscera and extend into the trunk and tail through the dorsal aortas and the vessels in the head. [17] Therefore, ^{13}C-QDs have potential for *in vivo* images with their easy transportation through cardiovascular system. Confocal images further confirmed that the ^{13}C-QDs accumulated on the eyeball selectively, but could not enter into the lens (Fig. 5), similar to the fluorescence result in Fig. 4H.

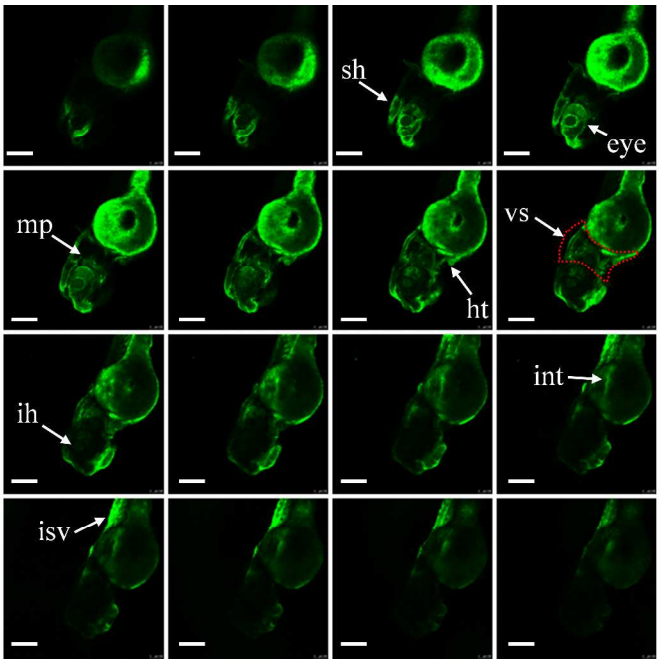

Fig. 5. Confocal images of zebrafish at different scan-planes. The eye, heart (ht), internal of head (ih), intestine (int), intersegmental vessel (isv), mesencephalon (mp), surface of head (sh), and viscera (vs) are clearly illustrated. Scale bar: 200 μm.

Experimental details

^{12}C- and ^{13}C-QDs were prepared by hydrothermal treatment of ^{12}C- or ^{13}C-glucose and monoethanolamine (MEA). Briefly, the ^{12}C- or ^{13}C-glucose (40 mg, 0.25 mmol) was mixed with 10 mL water and then added with 80 μL MEA. The mixture was added into a poly-tetrafluoroethylene (Teflon)-lined autoclave (30 mL) and heated at 200 °C for 12 h. The C-QDs was collected after filtering with 0.22 μm membrane and dialyzed against water.

The solution was lyophilized to obtain brown C-QDs pasty, which can be re-dissolved for use.

AB strain zebrafish were used in this study. All procedures using animals were approved by the Institutional Animal Care Committee of Nankai University. Zebrafish were maintained in aquaria at 28.5°C with a 10/14-hour dark/light cycle. Embryos were collected after natural spawns and housed at 28.5°C. The embryo and larva are staged by hour post fertilization (hpf). All embryos were grown in 0.003 %1-phenyl-2-thiourea (PTU, Sigma-Aldrich, St. Louis, MO, USA) to block pigmentation and mediate visualization until 72 hours post fertilization (hpf).

The cell viability was evaluated on the 4T1 cells using CCK8 assay. Briefly, the cell was seeded in 96-well culture plates at a density of 5×10^5 cells per well in culture medium. The C-QDs, diluted to the final concentration of 10, 100, 250, 500, 1000, 2000 and 3000 μg mL^{-1}, was introduced to cells for incubation of 8 and 24h after 4T1 cells reached 90-95% confluence. Cells cultured in the free medium were taken as positive control, while Triton x-100 was added to medium as negative control. 10 μL CCK-8 was added to each well, followed by the cells were incubated for another 1 h. The cell incubation process was carried out at 37 °C with 5% CO_2. The absorbance at 490 nm was measured for the calculation of the cell survival rate. The experiment was performed under identical conditions three times.

The 72 hpf zebrafish embryos were added into 24-well culture plates (5–7 zebrafish per well) and incubated with different concentration of ^{13}C-QDs (0, 0.1, 0.5, 1.5, 3, and 5 mg mL^{-1}) for 8 h. The zebrafish was collected to evaluate the *in vivo* biological toxicity of ^{13}C-QDs. All of the experiments were performed under identical conditions for five times.

The AB strain fertilized embryos were added in 24-well culture plates (5–7 of embryos per well) at 1–4 cell stage (less than 1 hour). The ^{13}C-QDs with concentration of 0, 1.0, 1.5, 3.0, and 5.0 mg mL^{-1} was introduced into wells. After cultured for 2 h in ^{13}C-QD solution, the embryos were rinsed with free tank water three times to remove excess ^{13}C-QDs. and fluorescent images of embryos were taken at 3, 7, 26, 32, 48, and 72 hpf by a Fluorescence microscope (Olympus BX51, Japan) with an excitation of 470-490 nm and emission at 515 nm long pass. The MR spectra were obtained with a 400 mHz nuclear magnetic resonance instrument (Bruck, Germany) after embryos were added into D_2O.

AB strain fertilized embryos were cultured in regular tank water at 28.5 °C until 3 days post fertilization (3 dpf, i.e. 72 hpf). The zebrafish at 72 hpf were added in 24-well culture plates (5–7 zebrafish per well). The ^{13}C-QDs were added to the wells with different concentration: 0, 0.1, 0.25, 0.5, 0.75, 1.5, and 3 mg mL^{-1}. After cultured for 8 h, zebrafish were rinsed with tank water three times to remove excess C-QDs, followed by the imaging with fluorescence microscope (Olympus BX51, Japan) with an excitation of 470–490 nm and emission at 515 nm long pass. The confocal imaging of the zebrafish was performed on a Leica Tcs sp5 confocal microscope (Germany) with the filter of excitation and emission at 488 nm and 520–620 nm, respectively.

The 72 hpf zebrafish embryos were added in 24-well culture plates and incubated with 3 mg mL^{-1} of ^{12}C- or ^{13}C-QDs. After cultured for 8 h, zebrafish were washed with tank water to remove excess C-QDs. The zebrafish was collected and then re-dissolved into D_2O to obtain the MR spectra of zebrafish with ^{12}C- or ^{13}C-QDs.

Conclusions

In summary, our ^{13}C-QDs constituted a novel MR and fluorescence dual-response probe to report biological process. ^{13}C-QDs showed ^{13}C-MR response even when they were embedded in zebrafish. This phenomenon has not yet been described previously. Compared with ^{13}C-labeled molecular probes, ^{13}C-QDs were ^{13}C-rich probe to enhance the MR signal and thus the complex setups for hyperpolarization were not required. Moreover, the lifetime of MR response was unlimited. Importantly, ^{13}C-QDs also kept their intrinsic fluorescence emission. The dual-response of ^{13}C-QDs was validated with a zebrafish model, where tissue-dependent affinity of ^{13}C-QDs was confirmed. The results obtained from zebrafish may be applied to study of other animals, so the multifunctional ^{13}C-QDs constitute a novel powerful tool for medical applications.

Acknowledgements

This work was supported by 973 Program of China (Grant No. 2011CB707703), the NSF of China (Grant Nos. 21375064, 81301080, 81250017), and National Key Technology R&D Program of China (Grant No. 2012BAI08B06).

Notes and references

[a] State Key Laboratory of Medicinal Chemical Biology, Collaborative Innovation Center of Chemical Science and Engineering (Tianjin), and Research Center for Analytical Sciences, College of Chemistry, Nankai University, Tianjin, 300071, China.

[b] Key Laboratory of Animal Models and Degenerative Neurological Diseases (Tianjin), School of Medicine, Nankai University, Tianjin, 300071, China.

[c] Dalian Institute of Chemical Physics, National Chromatographic R. & A. Center, Chinese Academy of Sciences, Dalian, 116011, China.

† Electronic Supplementary Information (ESI) available: [Characterization, quantum yields, upconverted emission, stability, and fluorescence imaging of C-QD]. See DOI: 10.1039/b000000x/

1 A. Louie, *Chem. Rev.* 2010, **110**, 3146-3195.

2 (a) T. Doura, R. Hata, H. Nonaka, K. Ichikawa, S. Sando, *Angew. Chem. Int. Ed.* 2012, **51**, 10114-10117; (b) A. R. Lippert, K. R. Keshari, J. Kurhanewicz, C. J. Chang, *J. Am. Chem. Soc.* 2011, **133**, 3776-3779.

3 (a) K. R. Keshari, D. M. Wilson, *Chem. Soc. Rev.* 2014, **43**, 1627-1659; (b) W. Wiechert, *Metab. Eng.* 2001, **3**, 195-206; (c) T. Niittylae, B. Chaudhuri, U. Sauer, W. B. Frommer, In *Methods Mol. Biol.* 2009, **553**, 355-372; (d) S. Radajewski, P. Ineson, N. R. Parekh, J. C. Murrell, *Nature* 2000, **403**, 646-649; e) S.-E. Ong, I. Kratchmarova, M. Mann, *J Proteome Res.* 2002, **2**, 173-181; (f) C. S. Ward, H. S. Venkatesh, M. M. Chaumeil, A. H. Brandes, M.

Vancriekinge, H. Dafni, S. Sukumar, S. J. Nelson, D. B. Vigneron, J. Kurhanewicz, C. D. James, D. A. Haas-Kogan, S. M. Ronen, *Cancer Res.* 2010, **70**, 1296-1305; (g) S. B. Duckett, R. E. Mewis, *Acc. Chem. Res.* 2012, **45**, 1247-1257; (h) S. Mansson, E. Johansson, P. Magnusson, C. M. Chai, G. Hansson, J. S. Petersson, F. Stahlberg, K. Golman, *Eur. Radiol.* 2006, **16**, 57-67; (i) M. J. Albers, R. Bok, A. P. Chen, C. H. Cunningham, M. L. Zierhut, V. Y. Zhang, S. J. Kohler, J. Tropp, R. E. Hurd, Y.-F. Yen, S. J. Nelson, D. B. Vigneron, J. Kurhanewicz, *Cancer Res.* 2008, **68**, 8607-8615.

4 (a) M. R. Smith, E. T. Peterson, J. W. Gordon, D. J. Niles, I. J. Rowland, K. N. Kurpad, S. B. Fain, *IEEE T. Bio-med. Eng.* 2012, **59**, 45-49; (b) M. C. D. Tayler, I. Marco-Rius, M. I. Kettunen, K. M. Brindle, M. H. Levitt, G. Pileio, *J. Am. Chem. Soc.* 2012, **134**, 7668-7671.

5 (a) U. Resch-Genger, M. Grabolle, S. Cavaliere-Jaricot, R. Nitschke, T. Nann, *Nat. Meth.* 2008, **5**, 763-775; (b) P. G. Luo, S. Sahu, S.-T. Yang, S. K. Sonkar, J. Wang, H. Wang, G. E. LeCroy, L. Cao, Y.-P. Sun, *J. Mater. Chem. B* 2013, **1**, 2116-2127; (c) L. Cao, M. J. Meziani, S. Sahu, Y.-P. Sun, *Acc. Chem. Res.* 2012, **46**, 171-180; (d) J. Wang, C.-F. Wang, S. Chen, *Angew. Chem. Int. Ed.* 2012, **51**, 9297-9301; (e) X. Xu, R. Ray, Y. Gu, H. J. Ploehn, L. Gearheart, K. Raker, W. A. Scrivens, *J. Am. Chem. Soc.* 2004, **126**, 12736-12737; (f) H. T. Li, X. D. He, Y. Liu, H. Huang, S. Y. Lian, S. T. Lee, Z. H. Kang, *Carbon* 2011, **49**, 605-609; (g) C. F. Wang, X. Wu, X. P. Li, W. T. Wang, L. Z. Wang, M. Gu, Q. Li, *J. Mater. Chem.* 2012, **22**, 15522-15525; (h) S. N. Baker; G. A. Baker, *Angew. Chem. Int. Ed.* 2010, **49**, 6726-6744; (i) Y. Xu, M. Wu, X.-Z. Feng, X.-B. Yin, X.-W. He, Y.-K. Zhang, *Chem. Eur. J.* **2013**, **19**, 6282-6288; (j) S.-T. Yang, X. Wang, H. Wang, F. Lu, P. G. Luo, L. Cao, M. J. Meziani, J.-H. Liu, Y. Liu, M. Chen, Y. Huang, Y.-P. Sun, *J. Phys. Chem. C* 2009, **113**, 18110-18114; (k) Z. Liu, X. Li, S. M. Tabakman, K. Jiang, S. Fan, H. Dai, *J. Am. Chem. Soc.* 2008, **130**, 13540-13541; (l) X. Wang, C. Wang, L. Cheng, S.-T. Lee, Z. Liu, *J. Am. Chem. Soc.* 2012, **134**, 7414-7422; (m) M. H. Rümmeli, M. Löffler, C. Kramberger, F. Simon, F. Fülöp, O. Jost, R. Schönfelder, A. Grüneis, T. Gemming, W. Pompe, B. Büchner, T. Pichler, *J. Phys. Chem. C* 2007, **111**, 4094-4098; (n) W. L. Wei, C. Xu, L. Wu, J. S. Wang, J. S. Ren, X. G. Qu, *Sci. Rep.* 2014, **4**, 2308; (o) L. M. Shen, M. L. Chen, L. L. Hu, X. W. Chen and J. H. Wang, *Langmuir*, 2013, **29**, 16135-16140; (p) H. P. Yan, M. Q. Tan, D. M. Zhang, F. S. Cheng, H. Wu, M. K. Fan, X. J. Ma and J. H. Wang, *Talanta*, 2013, **108**, 59-65.

6 C. Ding, A. Zhu, Y. Tian, *Acc. Chem. Res.* 2014, **47**, 20-30.

7 (a) Z. Ma, H. Ming, H. Huang, Y. Liu, Z. Kang, *New J. Chem.* 2012, **36**, 861-864; (b) H. Peng, J. Travas-Sejdic, *Chem. Mater.* 2009, **21**, 5563-5565; (c) H. Li, X. He, Y. Liu, H. Huang, S. Lian, S.-T. Lee, Z. Kang, *Carbon* 2011, **49**, 605-609.

8 (a) Y.-Q. Zhang, D.-K. Ma, Y. Zhuang, X. Zhang, W. Chen, L.-L. Hong, Q.-X. Yan, K. Yu, S.-M. Huang, *J. Mater. Chem.* 2012, **22**, 16714-16718; (b) J. Lu, J.-X. Yang, J. Wang, A. Lim, S. Wang, K. P. Loh, *ACS Nano* 2009, **3**, 2367-2375.

9 S. Zhu, Q. Meng, L. Wang, J. Zhang, Y. Song, H. Jin, K. Zhang, H. Sun, H. Wang, B. Yang, *Angew. Chem. Int. Ed.* 2013, **52**, 3953-3957.

10 L. Tian, D. Ghosh, W. Chen, S. Pradhan, X. Chang, S. Chen, *Chem. Mater.* 2009, **21**, 2803-2809.

11 J. Wang, C.-F. Wang, S. Chen, *Angew. Chem.* 2012, **124**, 9431-9435.

12 (a) S. K. Ko, X. Chen, J. Yoon, I. Shin, *Chem. Soc. Rev.* 2011, **40**, 2120-2130; (b) G. J. Lieschke, P. D. Currie, *Nat. Rev. Genet.* 2007, **8**, 353-367; (c) S. T. Laughlin, J. M. Baskin, S. L. Amacher, C. R. Bertozzi, *Science* 2008, **320**, 664-667; (d) J. M. Baskin, K. W. Dehnert, S. T. Laughlin, S. L. Amacher, C. R. Bertozzi, *Proc. Natl. Acad. Sci. USA* 2010, **107**, 10360-10365.

13 J. Cheng, E. Flahaut, S. H. Cheng, *Environ. Toxicol. Chem.* 2007, **26**, 708-716.

14 R. Handy, T. Henry, T. Scown, B. Johnston, C. Tyler, *Ecotoxicology* 2008, **17**, 396-409.

15 a) K. Howe, M. D. Clark, C. F. Torroja, J. Torrance, C. Berthelot, M. Muffato, J. E. Collins, S. Humphray, K. McLaren, L. Matthews, S. McLaren, I. Sealy, M. Caccamo, C. Churcher, C. Scott, J. C. Barrett, R. Koch, G. J. Rauch, S. White, W. Chow, B. Kilian, L. T. Quintais, J. A. Guerra-Assuncao, Y. Zhou, Y. Gu, J. Yen, J. H. Vogel, T. Eyre, S. Redmond, R. Banerjee, J. Chi, B. Fu, E. Langley, S. F. Maguire, G. K. Laird, D. Lloyd, E. Kenyon, S. Donaldson, H. Sehra, J. Almeida-King, J. Loveland, S. Trevanion, M. Jones, M. Quail, D. Willey, A. Hunt, J. Burton, S. Sims, K. McLay, B. Plumb, J. Davis, C. Clee, K. Oliver, R. Clark, C. Riddle, D. Eliott, G. Threadgold, G. Harden, D. Ware, B. Mortimer, G. Kerry, P. Heath, B. Phillimore, A. Tracey, N. Corby, M. Dunn, C. Johnson, J. Wood, S. Clark, S. Pelan, G. Griffiths, M. Smith, R. Glithero, P. Howden, N. Barker, C. Stevens, J. Harley, K. Holt, G. Panagiotidis, J. Lovell, H. Beasley, C. Henderson, D. Gordon, K. Auger, D. Wright, J. Collins, C. Raisen, L. Dyer, K. Leung, L. Robertson, K. Ambridge, D. Leongamornlert, S. McGuire, R. Gilderthorp, C. Griffiths, D. Manthravadi, S. Nichol, G. Barker, S. Whitehead, M. Kay, *Nature* 2013, **496**, 498-503; b) R. N. Kettleborough, E. M. Busch-Nentwich, S. A. Harvey, C. M. Dooley, E. de Bruijn, F. van Eeden, I. Sealy, R. J. White, C. Herd, I. J. Nijman, F. Fenyes, S. Mehroke, C. Scahill, R. Gibbons, N. Wali, S. Carruthers, A. Hall, J. Yen, E. Cuppen, D. L. Stemple, *Nature* 2013, **496**, 494-497.

16 P. J. Keller, *Science* 2013, **340**, 1184-1195.

17. P. J. Keller, *Methods*, 2013, **62**, 268-278.

